Supporting Information

Surface and Interface Porosity of Polymer/Fullerene-Derivative Thin Films Revealed by Contrast Variation of Neutron and X-ray Reflectivity

Heng-Jui Liu, [a,b] *U-Ser Jeng,* [a,*] *Norifumi L. Yamada,* [c] *An-Chung Su,* [d] *Wei-Ru Wu,* [a] *Chun-Jen Su,* [a] *Su-Jien Lin,* [b] *Kung-Hwa Wei,* [e] *and Mao-Yuan Chiu* [e]

[a] *National Synchrotron Radiation Research Center, Hsinchu 30076, Taiwan*
[b] *Department of Materials Science and Engineering, National Tsing Hua University, Hsinchu, 30013, Taiwan*
[c] *Neutron science Laboratory, High Energy Accelerator Research Organization, Tokai, Naka 319-1106, Japan.*
[d] *Department of Chemical Engineering, National Tsing Hua University, Hsinchu 30013, Taiwan.*
[e] *Department of Materials Science and Engineering, National Chiao Tung University, Hsinchu 30050, Taiwan.*

[*] *Corresponding author*
U-Ser Jeng
National Synchrotron Radiation Research Center
101 Hsin-Ann Road, Hsinchu Science Park,
Hsinchu 30076, Taiwan
Tel : +886-3-578-0281
Fax : +886-3-578-3813

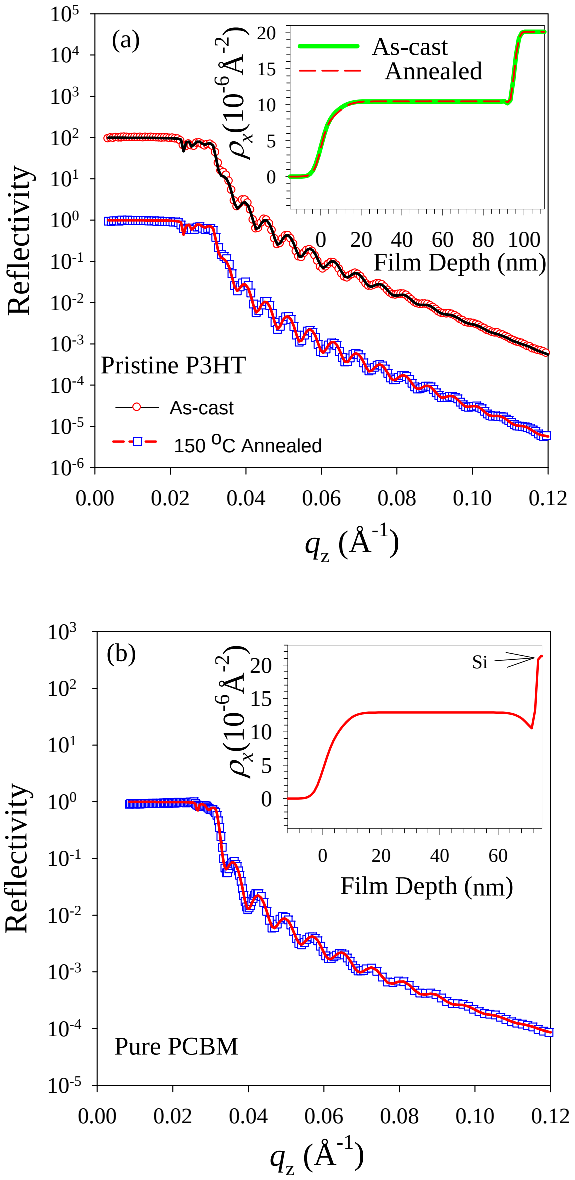

Fig. S1. X-ray reflectivity (XR) data for pure (a) P3HT and (b) PCBM films spun-cast on Si wafers. The data for the pristine P3HT film before and after 150 °C annealing are fitted (solid curves) with a single layer model of scattering-length-density (SLD) as shown in the inset. The SLD value for the film increased marginally from 10.20×10^{-6} Å^{-2} to 10.28×10^{-6} Å^{-2}, after annealing, corresponding to a marginal film density change from 1.10 ± 0.02 g cm^{-3} to 1.108 ± 0.02 g cm^{-3}. (b) The XR data for the pure PCBM film are fitted (solid curve) with a single layer model (inset) with a SLD value of 12.90×10^{-6} Å^{-2} , corresponding to a mean film density of 1.50 ± 0.05 g cm^{-3}.

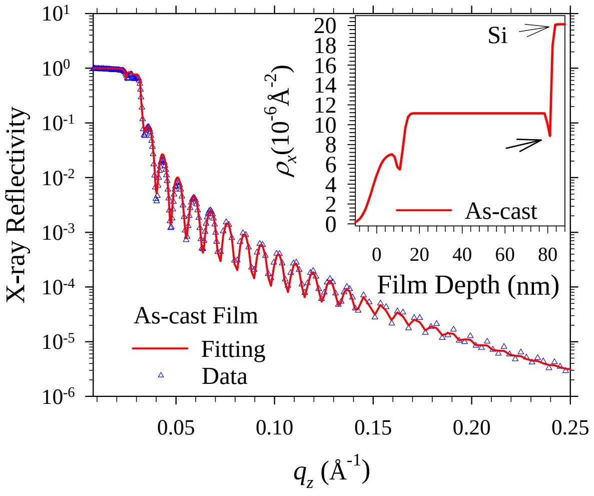

Fig. S2. X-ray reflectivity (XR) data for the as-cast P3HT/PCBM film on Si wafer (weight ratio of PCBM over P3HT c = 0.8). The data are fitted (solid curve) using the SLD (ρ_x) profile shown in the inset. Note the small dip (marked by an arrow) of the SLD near the interface may be responsible by PCBM (cf. Fig. S1) and could be largely remedied after 150 °C annealing for 15 min (cf. inset of Fig. 1a).

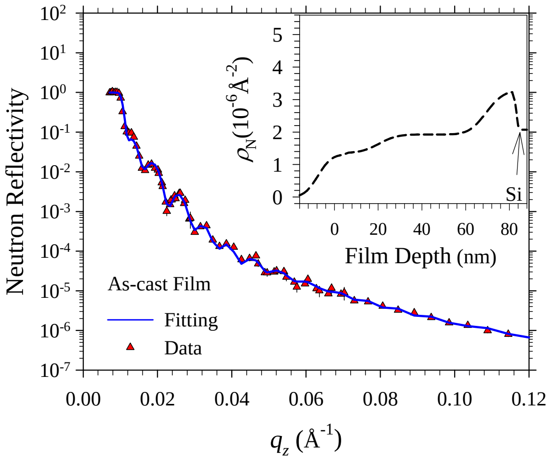

Fig. S3. Neutron Reflectivity (NR) data for the as-cast film of the same P3HT/PCBM (c = 0.8) film used for XR measurement. The data are fitted (solid curve) using the SLD profile ρ_N shown in the inset.

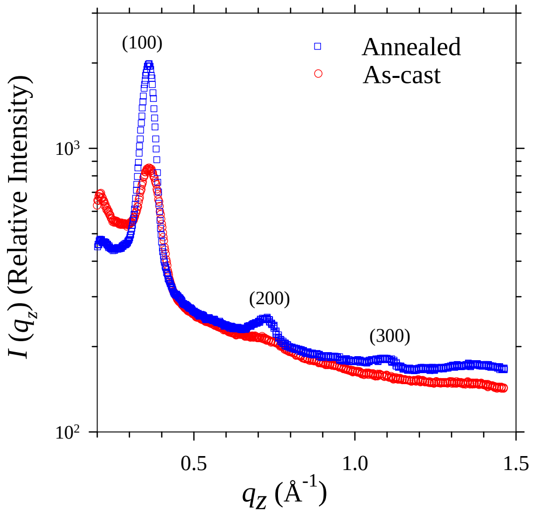

Fig. S4. GIWAXS data collected along the film normal direction (with the out-of-plane wavevector transfer q_z) for the as-cast and 150 °C annealed P3HT/PCBM films. Note the three significantly enhanced lamellar peaks (indexed) of P3HT after annealing, and the substantial (100) peak before annealing.

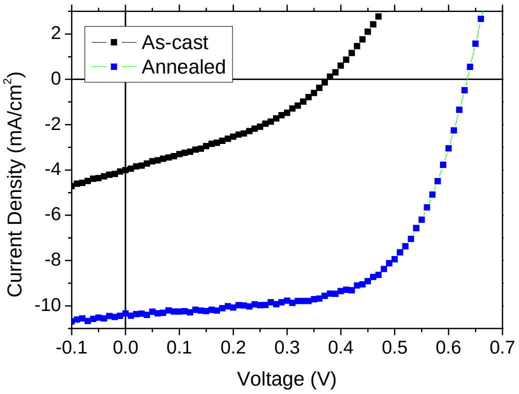

	PCE(%)	V_{oc}(V)	J_{sc} (mA/cm^2)	FF(%)
As-cast	0.5	0.38	4.0	35
150 °C Annealed	4.1	0.63	10.3	62

Fig. S5. Current density–voltage curves under illumination of the P3HT/PCBM devices with c = 0.8, prepared through as-cast and 150 °C annealing for 900 s, respectively. The corresponding device performance parameters are shown in the Table, with the power conversion efficiency PCE, open-circuit voltage V_{oc}, short-circuit current density J_{sc}, and fill factor FF.

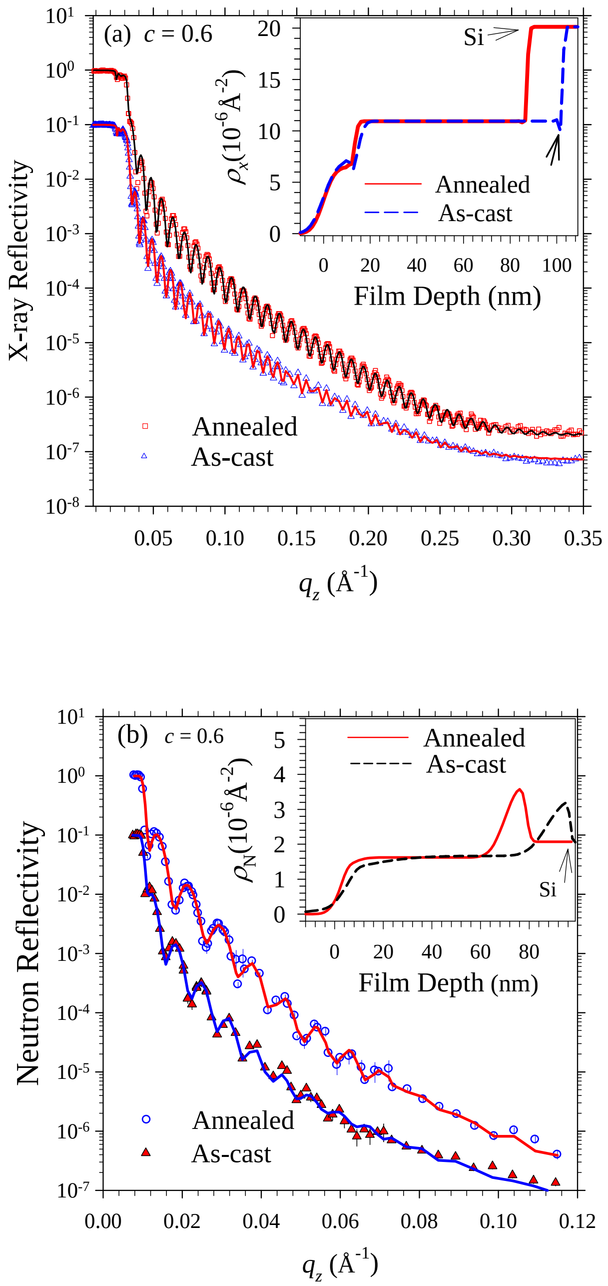

Fig. S6. XR (a) and NR (b) data for the 150 °C annealed and as-cast (data scaled down by a factor) P3HT/PCBM films with c = 0.6. The data are fitted (solid curves) using the corresponding SLD profiles shown in the insets. Note that the small dip of the X-ray SLD at the interface, marked by an arrow in the inset of (a), is healed after 150 °C annealing for 900 s. Note that the slightly different film thicknesses for the as-cast and annelaed films are resulted from some minor film processing uncertainty of different sample batches.

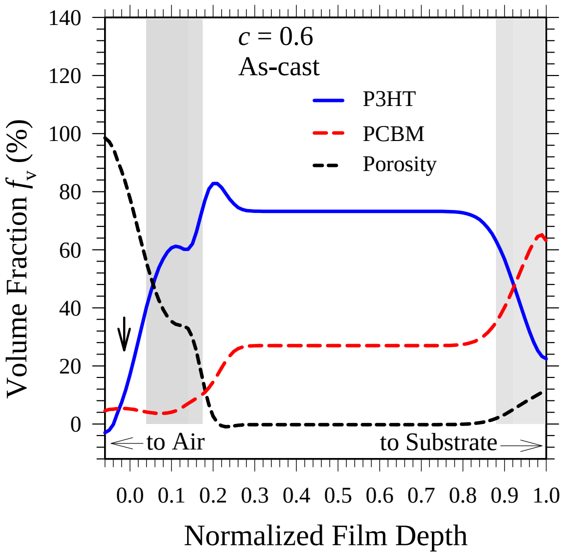

Fig. S7. Vertical volume fraction profiles of the PCBM, P3HT, and porosity of the as-cast P3HT/PCBM films with c = 0.6, obtained from the corresponding sets of contrast NR/XR SLD profiles shown in Fig. S6. Shaded areas highlight the surface and interface zones containing porosity. The thick arrow indicates the air-film transition (roughness) zone.

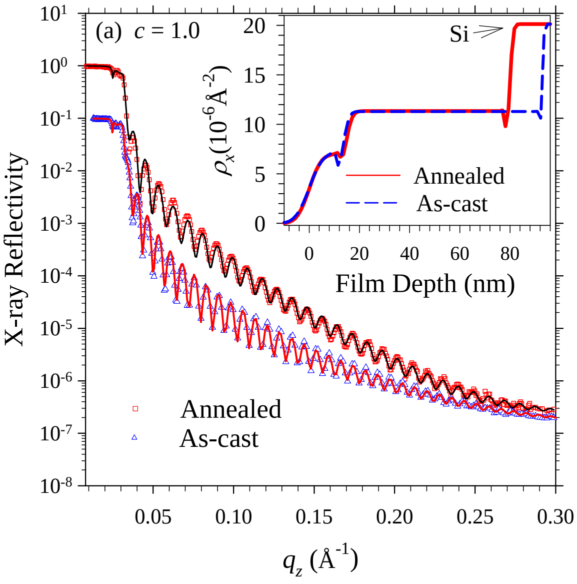

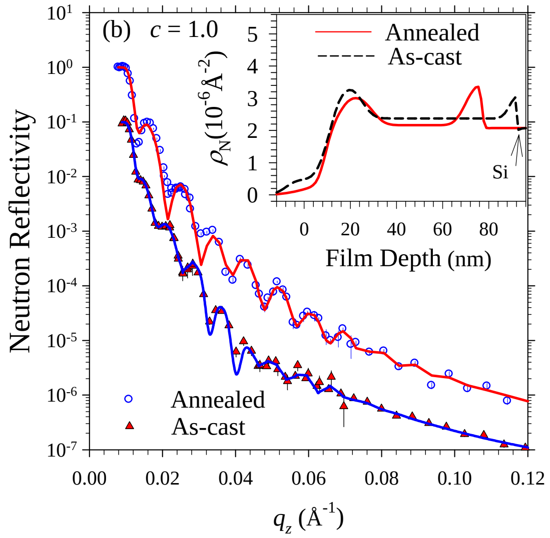

Fig. S8. XR (a) and NR (b) data for the 150 °C annealed and as-cast (data scaled down by a factor) P3HT/PCBM films with c = 1.0. The data are fitted (solid curves) using the corresponding SLD profiles shown in the insets.

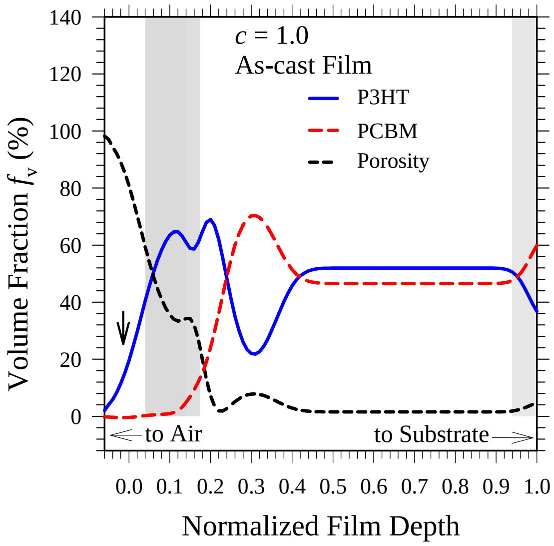

Fig. S9. Vertical volume fraction profiles of the PCBM, P3HT, and porosity of the as-cast P3HT/PCBM films with c = 1.0, obtained from the corresponding sets of contrast NR/XR SLD profiles shown in Fig. S8. Shaded areas highlight the surface and interface zones containing porosity. The thick arrow points to the air-film transition (roughness) zone. The sharper, unnatural transitions of the f_v profiles at z ~0.15 are resulted from the fine structural features of a few nanometers resolved by the XR data (cf. inset of Fig. S8a) but not by the NR data of a lower resolution owing to the relatively limited neutron data q_z-range (Fig. S8b).

GISAXS Data Analysis.

GISAXS intensity profiles in the lower-q region contributed by PCBM aggregates in the P3HT/PCBM blend were modeled by polydisperse spheres using

$$I(q) = \langle n_p \rangle \langle P(q) \rangle S(q), \qquad \text{(S1)}$$

with the averaged form factor $\langle P(q) \rangle$ and structure factor $S(q)$.[S1] The number density of the scattering particles $n_p(r) = \langle n_p \rangle f(r)$ is defined by the mean number density $\langle n_p \rangle$ and the Schultz size-distribution function[S2]

$$f(r) = \left(\frac{z+1}{r_a}\right)^{z+1} r^z \exp\left[-\left(\frac{z+1}{r_a}\right) r\right] / \Gamma(z+1), \qquad \text{(S2)}$$

with z > −1,

and the mean radius r_a, width parameter z, and polydispersity $p = (z+1)^{-1/2}$. The form factor for spheres $P(q) = [3 j_1(qr)/(qr)]^2$ is defined by the first-order spherical Bessel function $j_1(qr)$.[S3] For spheres with small polydispersity, $S(q)$ may be approximated by the structure factor of the effective one-component system of hard spheres,

$$S(q) = [1 - n_p C(q)]^{-1} \qquad \text{(S3)}$$

with the effective diameter σ and volume fraction ϕ.[S4] Here, $C(q) = 4\pi\sigma^3\xi^{-6} \{\alpha_o\xi^3 (\sin\xi - \xi\cos\xi) + \beta_o\xi^2 [2\xi\sin\xi - (\xi^2-2)\cos\xi - 2] + \gamma [(4\xi^3-24\xi)\sin\xi - (\xi^4 - 12\xi + 24)\cos\xi + 24]\}$ is defined by $\xi = q\sigma$, $\alpha_o = (1+2\phi)^2 (1-\phi)^{-4}$, $\beta_o = -6\phi\, [1+(\phi/2)]^2 (1-\phi)^{-4}$, and $\gamma = \phi\alpha_o/2$.

The GISAXS data fitting results shown in Fig. 4 include an additional term described by the Debye-Buche correlation function,[S5] $I(q) = (1+q^2\zeta^2)^{-2}$ to account for the relatively sharp upturn scattering in the very low-q region 0.005–0.007 Å^{-1}. The Debye-Buche correlation lengths, ζ, fitted for the as-cast and annealed film are about the same (60 ± 10 nm), and are attributed to P3HT fibrils [Ref. .12].

References

S1. S.-H. Chen and T.-L. Lin, *Methods of Experimental Physics—Neutron Scattering in Condensed Matter Research*; Eds. Sköld, K.; Price, D. L. Academic Press: New York, **1987**; Vol. 23B, Ch. 16.

S2 E. Y. Sheu, *Phys. Rev.* A, 1992, ***45,*** 2428.

S3 J. B. Hayter and J. Penfold, *Mol. Phys.* 1981, ***42***, 109.

S4 C. H. Su, U. Jeng, S. H. Chen, S. J. Lin, W. R. Wu, W.-T. Chuang, J. C. Tsai, A. C. Su, *Macromolecules* 2009, ***42***, 6656.

S5 Debye, P., Jr.; Anderson, H. R.; Brumberger, H. Scattering by An Inhomogeneous Solid. II. The Correlation Function and Its Application. *J. Appl. Phys.* 1957, **28**, 679.